PERGAMON

International Journal of Heat and Mass Transfer 44 (2001) 4649–4665

International Journal of HEAT and MASS TRANSFER

www.elsevier.com/locate/ijhmt

An investigation of a block moving back and forth on a heat plate under a slot jet. Part II (the effects of block moving distance and vacant distance)

Wu-Shung Fu *, Ke-Nan Wang

Department of Mechanical Engineering, National Chiao Tung University, 1001 Ta Hsueh Road, Hsinchu 30010, Taiwan, ROC

Received 28 November 2000; received in revised form 28 February 2001

Abstract

A continuous investigation of a block moving back and forth on a heat plate under a slot jet was studied numerically. This study investigates the effects of block moving distance and vacant distance between the block and heat plate on the heat transfer of heat plate. This subject belongs to a kind of moving boundary problems, and the modified Arbitrary Lagrangian Eulerian (ALE) method is suitable for solving this subject. The results show that the increment of the heat transfer rate of heat plate is not direct proportion to the block moving distance, and the smaller vacant distance is expected for obtaining the larger heat transfer rate of heat plate.

1. Introduction

Up to now, numerous methods have been proposed to enhance heat transfer rate of a heat body. These methods, which mainly included the passive and active methods, were summarized and reviewed in detail by Bergles [1,2]. A jet impingement is one of the above active methods and widely used as the cooling apparatus for high heat flux system such as electric cooling and turbine blade cooling. However, accompanying with the progress of semiconductor technology, the more compact device is produced indefatigably. The heat generated by the new device is always several times of the former one and becomes the main defect of the failure of device. As a result, how to increase the heat transfer rate of the jet impingement becomes a very important issue.

In the past, Mujumdar and Douglas [3], Martin [4], and Jambunathan et al. [5] reviewed the contemporary literature about the jet impingement system. Chou and Hung [6] studied fluid flow and heat transfers of a confined slot jet numerically and found that the Nusselt number at the stagnation line was proportional to jet Reynolds number in a 0.5 power and the ratio of separation distance to jet width in a −0.17 power. Chakroun et al. [7] investigated heat transfer of a round air jet impinging normally on a heated rough surface and found that the local and average Nusselt numbers of a rough surface were larger than those of a smooth surface by 8.9–28%. Chung et al. [8] investigated heat transfer characteristics of an axisymmetric jet impinging on a rib-roughened convex surface. The average Nusselt numbers on the rib-roughened convex surface were more than those on the smooth surface by 14–34%. Besides, in several experimental studies, an extra mechanism in the jet impingement system was installed to enhance the heat transfer rate of the jet impingement. Zumbrunnen and Aziz [9] investigated an intermittent water jet impinging on a constant heat flux surface experimentally, and found that the enhancement of heat transfer rate occurred as the frequency of the intermittence was sufficiently high enough. Haneda et al. [10] enhanced heat transfer rate of a jet impingement by inserting a suspended cylinder between the jet exit and the heat plate. The oscillation of the cylinder vibrated the flow field, and the maximum Nusselt number around the stagnation point was augmented about 20% compared with that without the insertion of a cylinder.

* Corresponding author. Tel.: +886-3-5712121 ext. 55110; fax: +886-3-572-0634.

E-mail address: wsfu@cc.nctu.edu.tw (W.-S. Fu).

0017-9310/01/$ - see front matter
PII: S0017-9310(01)00110-7

Nomenclature

b	dimensional width of the block (m)
d	dimensional vacant distance (m)
D	dimensionless vacant distance
h	dimensional height of the block (m)
H	dimensional height of the channel (m)
L	dimensional length of the channel (m)
n	normal vector of surface
Nu	Nusselt number
p	dimensional pressure (N m^{-2})
p_∞	dimensional reference pressure (N m^{-2})
P	dimensionless pressure
Pr	Prandtl number
r	dimensional block moving distance (m)
R	dimensionless block moving distance
Re	Reynolds number
t	dimensional time (s)
T	dimensional temperature (K)
u, v	dimensional velocities in x- and y-directions (m s^{-1})
U, V	dimensionless velocities in X- and Y-directions
W	dimensional width of slot (m)
x, y	dimensional Cartesian coordinates (m)
X, Y	dimensionless Cartesian coordinates

Greek symbols

α	thermal diffusivity (m^2 s^{-1})
δ	dimensional boundary layer thickness (m)
θ	dimensionless temperature
λ	penalty parameter
ν	kinematic viscosity (m^2 s^{-1})
ρ	dimensional density (kg m^{-3})
τ	dimensionless time

Subscripts

0	airflow inlet
b	block
h	heat plate
j	jet
s	stagnation line
x	local

Superscripts

$\bar{}$	mean value
$\hat{}$	grid

From the above literature, the increment of heat transfer rate of the jet impingement seems to have limitation in spite of installing any extra equipment. This could be the velocity and thermal boundary layers, which are disadvantageous to the heat transfer rate, are still on the heat plate. Consequently, as the huge enhancement of heat transfer rate is expected, the boundary layers mentioned above are necessarily destroyed. Fu et al. [11] first studied the heat transfer rate of a heat plate with a block moving back and forth on it under a slot jet numerically. The results showed that the moving block destroyed the boundary layer, and the new boundary layer reformed right after the moving block passing through. Based upon the reformation of new boundary layer, the maximum increment of heat transfer rate was about 200% in the largest velocity case. However, due to the limitation of contents of [11], the results about the effects of the vacant distance between block and plate and the block moving distance on the heat transfer of heat plate are incomplete.

Therefore, the aim of the study is to continue the investigation of the previous study [11] of a block moving back and forth on a heat plate under a slot jet. The effects of the vacant distance between block and plate and the block moving distance on the heat transfer of heat plate are mainly focused in the study. The problem belongs to a kind of moving boundary problems, and the Arbitrary Lagrangian Eulerian (ALE) method modified by Fu and Yang [12] is suitably adopted to solve this problem. The results show that the increment of the heat transfer rate of heat plate is not directly proportional to the block moving distance. And the larger enhancement of heat transfer rate can be obtained under the vacant distance between the moving block and heat plate being equal to or small than 0.01.

2. Physical model

The physical model is shown in Fig. 1. A two-dimensional channel with length L and height H is used to simulate the confined air jet impingement system. The air, which has uniform velocity v_0 and low temperature T_0, flows into the channel from a slot BC with width W, and impinges normally on the heat plate FK with high temperature T_h. The heat plate is as wide as the slot jet. The other surfaces of the channel (surfaces AB, CD, EF and KL) are insulated. An insulated moving block GHIJ with height h and width b is above the heat plate with a distance d, and moves back and forth in the region MN on the heat plate with a constant velocity u_b.

Initially ($t = 0$), the block is stationary at the middle position above the heat plate, and the flow field in the channel is steady. As time $t > 0$, the block starts to move with the constant velocity $-u_b$. When the point G of the block reaches the left point M on the heat plate, the block turns back instantly and moves to the right side with the constant velocity u_b. Similarly, when the point J

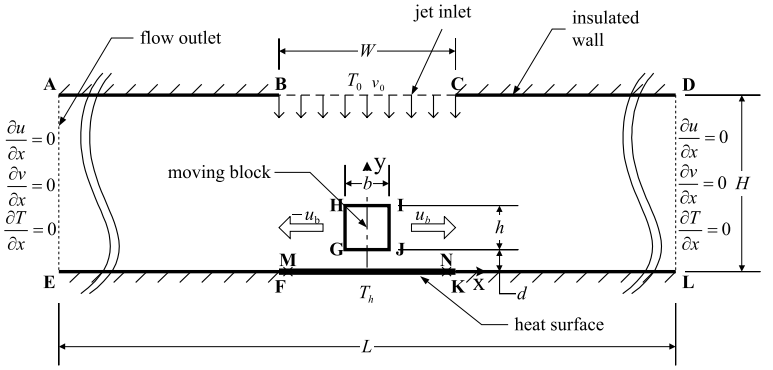

Fig. 1. Physical model.

of the block reaches the right point N on the heat plate, the block turns back immediately and moves to the left side with the constant velocity $-u_b$. The reciprocation motion of the block mentioned above is continuously executed. The boundary layer on the heat plate is destroyed by the moving block and a new boundary layer reforms right after as the block passes through. Consequently, the behaviors of both flow and thermal fields become time-dependent and can be categorized into a kind of moving boundary problems. As a result, the ALE method is properly utilized to analyze this problem.

For attaining the optimal heat transfer rate, the non-dimensional nozzle-to-plate spacing H/W was about 2.5 recommended by Chou and Hung [6]. Besides, in order to enhance the heat transfer rate effectively, the height of block must be greater than the thickness of the boundary layer to destroy the boundary layer completely. The non-dimensional boundary layer thickness (δ/W) is proportional to the jet Reynolds number in a 0.5 power and the non-dimensional nozzle-to-plate spacing in a 0.17 power [6]. As a result, when the jet Reynolds number is equal to 100, the dimensionless thickness of boundary layer δ/W is about 0.24, the height of block is then determined as $0.3W$.

To simplify the analysis, the following assumptions and the dimensionless variables are made.

1. The flow field is two-dimensional and laminar.
2. The fluid is Newtonian and incompressible.
3. The fluid properties are constant:

$$
\begin{aligned}
&X=\frac{x}{W}, \quad Y=\frac{y}{W}, \quad R=\frac{r}{W}, \quad D=\frac{d}{W},\\
&U=\frac{u}{v_0}, \quad V=\frac{v}{v_0}, \quad \hat{U}=\frac{\hat{u}}{v_0}, \quad U_b=\frac{u_b}{v_0},\\
&P=\frac{p-p_\infty}{\rho v_0^2}, \quad \tau=\frac{tv_0}{W}, \quad \theta=\frac{T-T_0}{T_h-T_0},\\
&Re_j=\frac{v_0 W}{\nu}, \quad Pr=\frac{\nu}{\alpha}.
\end{aligned}
\tag{1}
$$

Based upon the above assumptions and dimensionless variables, the dimensionless ALE governing equations (2)–(5) are expressed as the following equations:

Continuity equation:

$$\frac{\partial U}{\partial X}+\frac{\partial V}{\partial Y}=0. \tag{2}$$

Momentum equations:

$$
\begin{aligned}
&\frac{\partial U}{\partial \tau}+(U-\hat{U})\frac{\partial U}{\partial X}+V\frac{\partial U}{\partial Y}\\
&\quad=-\frac{\partial P}{\partial X}+\frac{1}{Re_j}\left(\frac{\partial^2 U}{\partial X^2}+\frac{\partial^2 U}{\partial Y^2}\right)
\end{aligned}
\tag{3}
$$

$$
\begin{aligned}
&\frac{\partial V}{\partial \tau}+(U-\hat{U})\frac{\partial V}{\partial X}+V\frac{\partial V}{\partial Y}\\
&\quad=-\frac{\partial P}{\partial Y}+\frac{1}{Re_j}\left(\frac{\partial^2 V}{\partial X^2}+\frac{\partial^2 V}{\partial Y^2}\right).
\end{aligned}
\tag{4}
$$

Energy equation:

$$\frac{\partial \theta}{\partial \tau}+(U-\hat{U})\frac{\partial \theta}{\partial X}+V\frac{\partial \theta}{\partial Y}=\frac{1}{Pr\,Re_j}\left(\frac{\partial^2 \theta}{\partial X^2}+\frac{\partial^2 \theta}{\partial Y^2}\right). \tag{5}$$

As $\tau>0$, the boundary conditions are as follows:

On the surfaces AB, CD, EF and KL

$$U=V=0, \quad \frac{\partial \theta}{\partial n}=0. \tag{6}$$

On the inlet slot surface BC

$$U=0, \quad V=-1, \quad \theta=0. \tag{7}$$

On the heat plate FK

$$U=V=0, \quad \theta=1. \tag{8}$$

On the outlet surfaces AE and DL

$$\frac{\partial U}{\partial n}=\frac{\partial V}{\partial n}=\frac{\partial \theta}{\partial n}=0. \tag{9}$$

On the surfaces of the block GH, HI, IJ and JG

$$U = u_b, \quad V = 0, \quad \frac{\partial \theta}{\partial n} = 0. \tag{10}$$

3. Numerical method

A Galerkin finite element method with moving grids and a backward scheme dealing with the time differential terms are adopted to solve the governing equations (2)–(5). A penalty function and Newton–Raphson iteration algorithm are utilized to reduce the pressure and nonlinear terms in the momentum equations, respectively. The velocity and temperature terms are expressed as quadrilateral and nine-node quadratic isoparametric elements. The discretization processes of the governing equations are similar to those used in [12]. Then the momentum equations (3) and (4) can be expressed as follows:

$$\sum_{1}^{n_e} \left([A]^{(e)} + [K]^{(e)} + \lambda [L]^{(e)} \right) \{q\}^{(e)}_{\tau+\Delta\tau} = \sum_{1}^{n_e} \{f\}^{(e)} \tag{11}$$

in which

$$\left(\{q\}^{(e)}_{\tau+\Delta\tau} \right)^{\mathrm{T}} = \langle U_1, U_2, \ldots, U_9, V_1, V_2, \ldots, V_9 \rangle^{m+1}_{\tau+\Delta\tau}, \tag{12}$$

where $[A]^{(e)}$ includes the (m)th iteration values of U and V at time $\tau + \Delta\tau$; $[K]^{(e)}$ includes the shape function, $\hat{U}$ and time differential terms; $[L]^{(e)}$ includes the penalty function terms; $\{f\}^{(e)}$ includes the known values of U and V at time τ and (m)th iteration values of U and V at time $\tau + \Delta\tau$.

After the flow field is solved, the energy equation (5) can be expressed as follows:

$$\sum_{1}^{n_e} \left([M]^{(e)} + [Z]^{(e)} \right) \{c\}^{(e)}_{\tau+\Delta\tau} = \sum_{1}^{n_e} \{r\}^{(e)}, \tag{13}$$

where

$$\left(\{c\}^{(e)}_{\tau+\Delta\tau} \right)^{\mathrm{T}} = \langle \theta_1, \theta_2, \ldots, \theta_9 \rangle_{\tau+\Delta\tau} \tag{14}$$

in which $[M]^{(e)}$ includes the values of U and V at time $\tau + \Delta\tau$; $[Z]^{(e)}$ includes the shape function, $\hat{U}$ and time differential terms; $\{r\}^{(e)}$ includes the known values of θ at time τ.

The value of penalty parameter used in the present study is 10^6 and the frontal method solver is utilized to solve Eqs. (11) and (13). The value of Prandtl number is equal to 0.71 for air. The grid velocity $\hat{U}$ is linear distribution and inverse proportion to the distance between the nodes and the moving block.

A brief outline of the solution procedure is described as follows:

1. Determine the optimal grid distribution and number of the elements and the nodes.
2. Solve the values of the U, V and θ at the steady state and regard them as the initial values.
3. Determine the moving velocity u_b of the block, the time increment $\Delta\tau$ and the grid velocities $\hat{U}$ of every node.
4. Update the coordinates of the nodes and examine the determinant of the Jacobian transformation matrix to ensure the one-to-one mapping to be satisfied during the Gaussian quadrature numerical integration, otherwise execute the mesh reconstruction.
5. Solve Eqs. (11) and (13), until the following criteria for convergence are satisfied:

$$\left| \frac{\varphi^{m+1} - \varphi^m}{\varphi^{m+1}} \right|_{\tau+\Delta\tau} < 10^{-3}, \quad \text{where } \varphi = U, V. \tag{15}$$

6. Continue the next time step calculation until the assigned time reaches.

For the thermal field, the energy balance is checked for every time step by the following equation:

$$E\,(\%) = \left[\left\{ \int_{\mathrm{FK}} Nu_x^{n+1}\,\mathrm{d}X - \int_{\mathrm{AE+DL}} Pr \cdot Re \cdot U^{n+1} \cdot \theta^{n+1}\,\mathrm{d}Y - \frac{Pr \cdot Re_j \cdot A \cdot \left(\overline{\theta}^{n+1} - \overline{\theta}^{n} \right)}{\mathrm{d}\tau} \right\} \Big/ \int_{\mathrm{FK}} Nu_x^{n+1}\,\mathrm{d}X \right] \times 100, \tag{16}$$

where

$$\int_{\mathrm{FK}} Nu_x^{n+1}\,\mathrm{d}X$$

is the thermal energy added into the system from the heat plate,

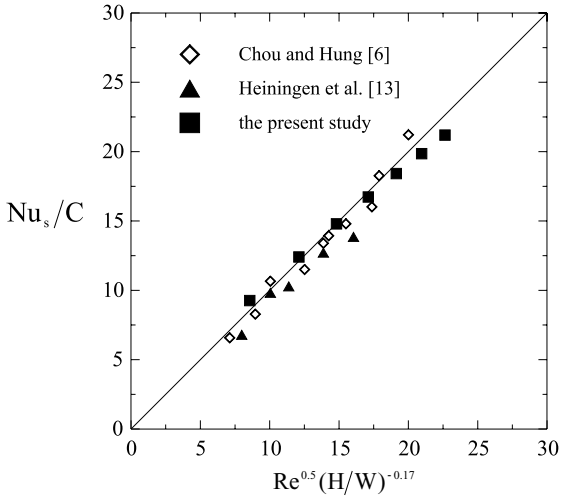

Fig. 2. Comparison of the results of the present study with those of Chou and Hung [6] and Heiningen et al. [13].

$$\int_{\mathrm{AE+DL}} Pr \cdot Re_{\mathrm{j}} \cdot U^{n+1} \cdot \theta^{n+1}\,\mathrm{d}Y$$

the thermal energy leaving the system with the fluid,

$$\frac{Pr \cdot Re_{\mathrm{j}} \cdot A \cdot \left(\overline{\theta}^{n+1} - \overline{\theta}^{n}\right)}{\mathrm{d}\tau}$$

the increment of the internal energy and

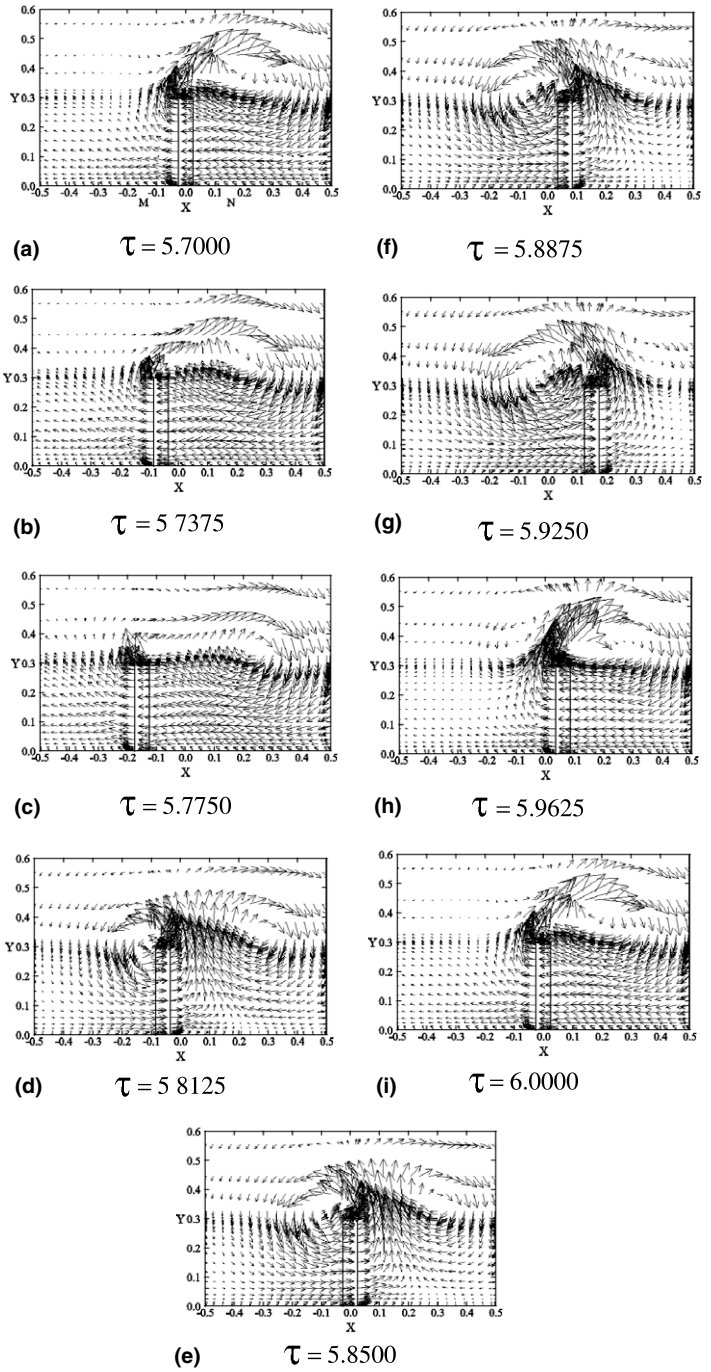

Fig. 3. The velocity vectors near the moving block for $R = 0.3$ under $Re_{\mathrm{j}} = 100$, $U_{\mathrm{b}} = 2.0$ and $D = 0.0$ cases.

$$Nu_x = -\left.\frac{\partial\theta}{\partial Y}\right|_{Y=0}$$

is the local Nusselt number.

The mesh and dimensionless time interval are tested for all cases. The stagnation Nusselt number was defined as the following equation by Chou and Hung [6].

$$Nu_s = C\,Re^{0.5}(H/W)^{-0.17}, \tag{17}$$

where C is 0.574 for the confined slot jet.

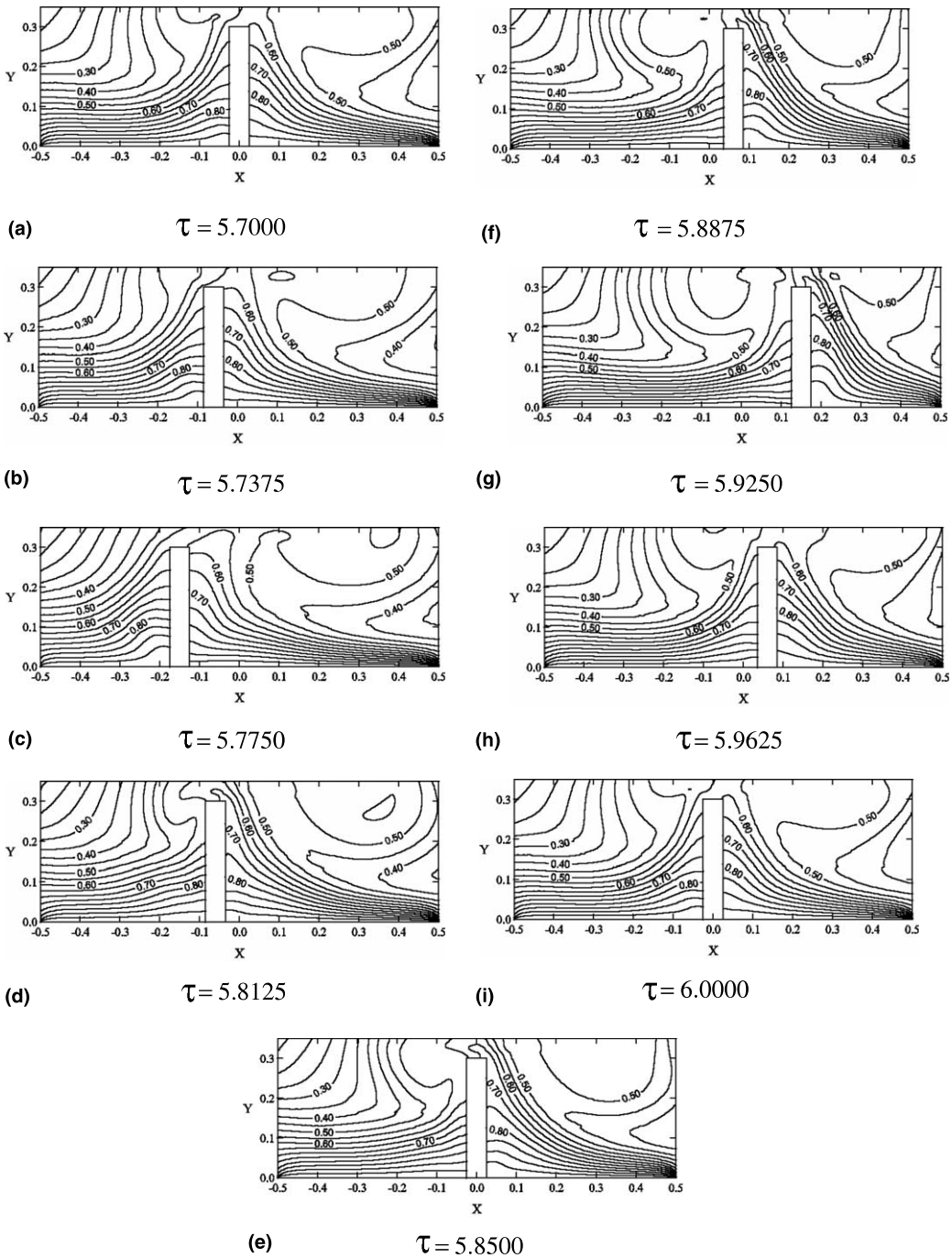

Fig. 4. The constant thermal lines near the moving block for $R = 0.3$ under $Re_j = 100$, $U_b = 2.0$ and $D = 0.0$ cases.

Shown in Fig. 2 the stagnation Nusselt numbers of the present study are compared with the results of Chou and Hung [6] and Heiningen et al. [13], and the deviation is slight.

4. Results and discussion

As the block moved on the heat plate (the vacant distance $D = 0$), the boundary layer on the heat plate

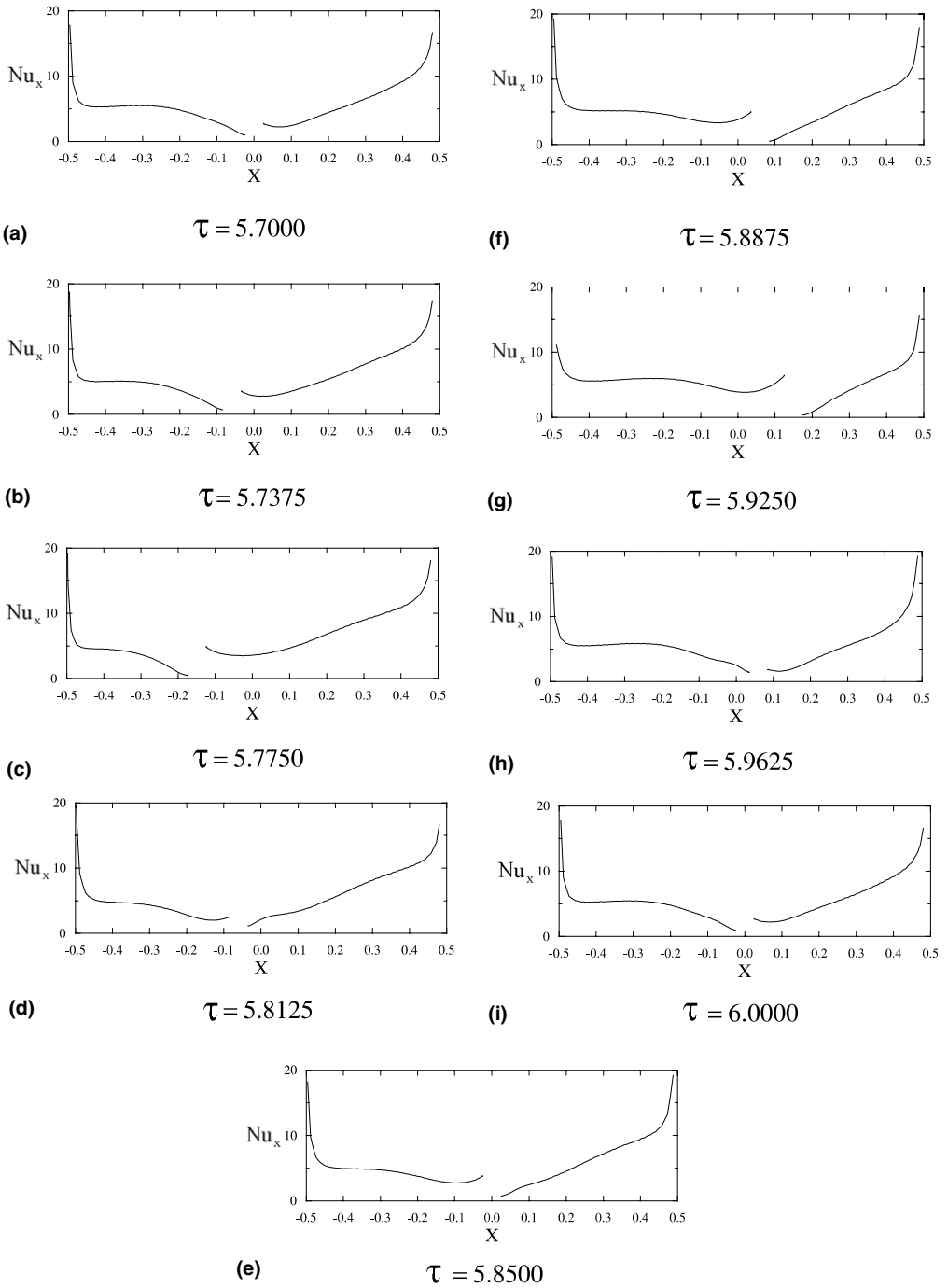

Fig. 5. The distributions of local Nusselt numbers on the heat plate for $R = 0.3$ under $Re_j = 100$, $U_b = 2.0$ and $D = 0.0$ cases.

before the moving block was destroyed and reformed immediately as the moving block passed through. More fluids, induced by the recirculation zone behind the moving block, flowed toward the heat plate. As a result, the heat transfer rate of the heat plate increased remarkably as shown in the previous study [11]. However, the results of the effects of block moving distance (R) and vacant distance (D) between the block and heat plate on the heat transfer of heat plate are inadequate in the above study. Then, in the present study, three block moving distances of $R = 0.3$, 0.6 and 0.9 and the vacant distances $D = 0.0$, 0.01 and 0.05 are investigated. For clearly indicating the phenomena around the block, only the flow and thermal fields close to the moving block are illustrated in the following figures.

4.1. Block moving distance (R)

The variations of the velocities, constant thermal lines and local Nusselt numbers for $R = 0.3$ under $Re_j = 100$, $U_b = 2.0$, and $D = 0.0$ are indicated in Figs. 3–5, respectively. These phenomena shown in Figs. 3–5 are in a certain period of total reciprocation motions.

The velocity vectors near the moving block are shown in Fig. 3. When the block moves leftward (Figs. 3(a)–(c)), the fluids before the moving block are pushed by the block and also flow leftward. The velocities of the fields close to the moving block are much larger than those of the fluids far away form the moving block. The original velocity boundary layer before the moving block is destroyed by the moving block. On the right surface of the block, the fluids complement the vacant

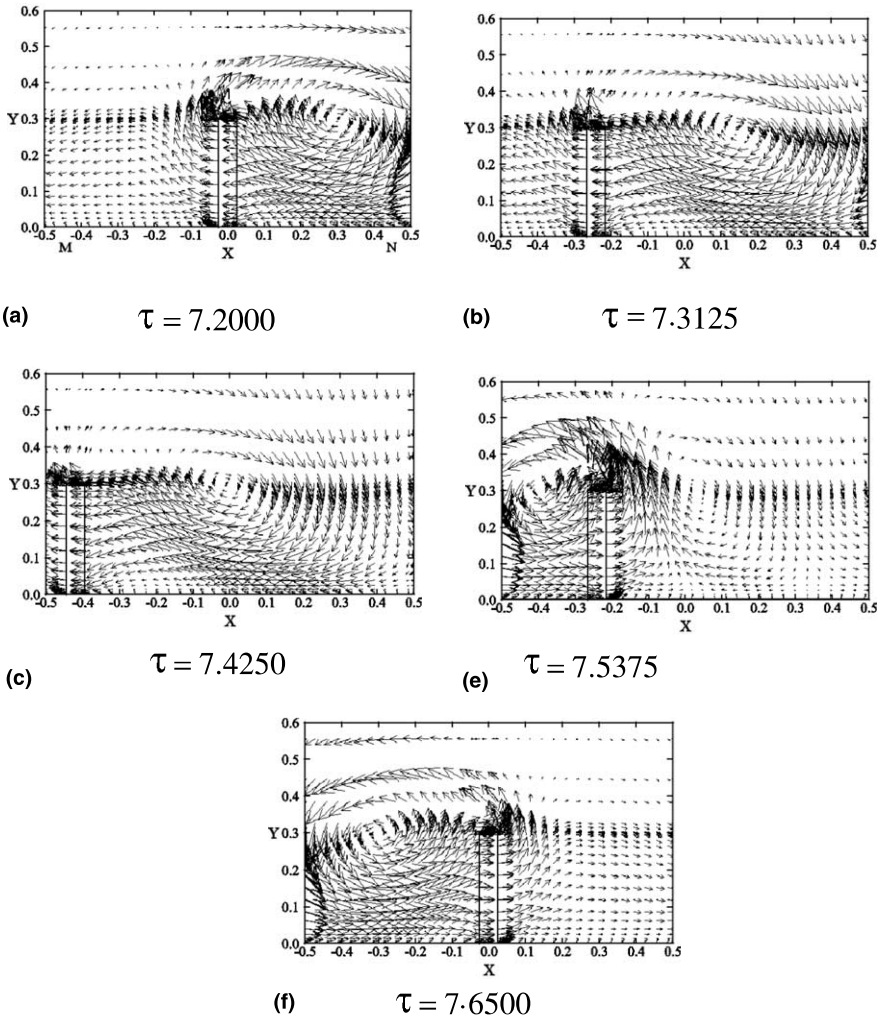

Fig. 6. The velocity vectors near the moving block for $R = 0.9$ under $Re_j = 100$, $U_b = 2.0$ and $D = 0.0$ cases.

space induced by the moving block, and the directions of these fluids are to the left. As a result, a new velocity boundary layer reforms immediately along the heat plate behind the moving block. The values of the velocities in the above new boundary layer are apparently larger than those in the original boundary layer shown in the left side of the block, and the increment of the velocities is beneficial to heat transfer rate. As the block continuously moves leftward, the formation of recirculation zone behind the moving block induces more fluids to flow toward the heat plate.

When the block moves rightward from the left point M to the right point N of the heat plate (Figs. 3(c)–(g)), the block pushes the fluids before the block to flow rightward. However, the fluids far away from the block flow leftward. Then the fluids before the moving block flow upward, and an interaction zone exists on the heat plate. Behind the moving block, the fluids flow rightward to fill the vacant space induced by the motion of block and form a recirculation zone. Accompany with the movement of the block, the recirculation zone behind the block develops continuously.

The block moves leftward immediately when the block reaches the right point N of the heat plate. The structures of the flow field shown in Figs. 3(h) and (i) are similar to those shown in Figs. 3(a) and (b). While the block reaches the center point of the heat plate (Fig. 3(i)), the flow field is similar to that shown in Fig. 3(a).

Figs. 4(a)–(i) show the distributions of constant thermal lines under the same conditions shown in Figs. 3(a)–(i), respectively. The thermal fields represent the characteristics of the flow fields. The thermal boundary layer on the heat plate before the moving block is destroyed by the block and reforms immediately as the block passes through. As a result, the distributions of constant thermal lines are sparse in front of the moving block and dense in back of the moving block. The new thermal boundary layer reforming behind the moving block causes the increment of heat transfer of the heat plate to be remarkable.

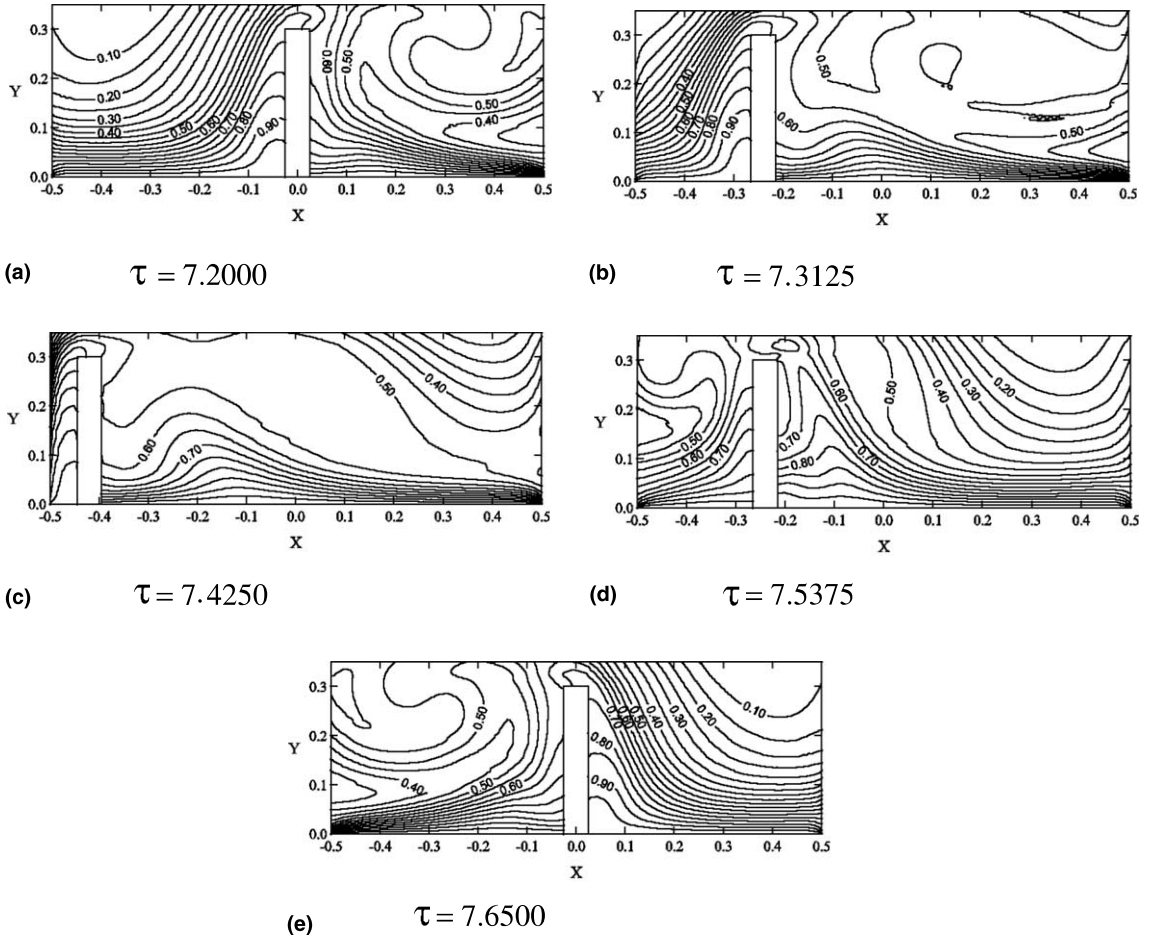

Fig. 7. The constant thermal lines near the moving block for $R = 0.9$ under $Re_j = 100$, $U_b = 2.0$ and $D = 0.0$ cases.

The distributions of local Nusselt number Nu_x are shown in Figs. 5(a)–(i) at the same conditions shown in Figs. 4(a)–(i), respectively. Due to the insulation of the block, the distributions of local Nusselt number shown in these figures are interrupted. The moving block pushes the fluids near the front surface of moving block, and the local Nusselt number becomes extremely small. Oppositely, the thermal boundary layer reforms behind the moving block, that leads the local Nusselt number to be large apparently. Away from the back surface of the moving block, the fluids induced by the moving block flow toward the heat plate that is beneficial to the heat transfer rate of heat plate, and the local Nusselt number becomes large.

The variations of the velocities, constant thermal lines and local Nusselt numbers for $R = 0.9$ under $Re_j = 100$, $U_b = 2.0$, and $D = 0.0$ are indicated in Figs. 6–8, respectively. The characteristics of the flow and thermal fields shown in Figs. 6–8 are similar to those shown in Figs. 3. However, in case $R = 0.9$, more fluids are induced by the moving block because of the larger block moving distance. The constant thermal lines are dense, and the local Nusselt number is large behind the moving block. At the same time, the flow and thermal fields shown in Figs. 6(a) and 7(a) are similar to those shown in Figs. 6(e) and 7(e), respectively, and the flow and thermal fields become periodic.

The variations of the average Nusselt number $\overline{Nu_x}$ of the heat plate as shown in Fig. 9 are at periodic state for $R = 0.3$, 0.6 and 0.9 cases. The average Nusselt number $\overline{Nu_x}$ is defined as the following equation:

$$\overline{Nu}_x = \int_{\text{heat plate}} Nu_x \, dX, \tag{18}$$

where the dimensionless length of the heat plate equals to 1.

The conditions of points a–i in Fig. 9(a) and a–e in Fig. 9(c) are the same conditions as Figs. 3–5 and 6–8, respectively.

As the block moves on the heat plate, the local Nusselt number usually decreases before the block and

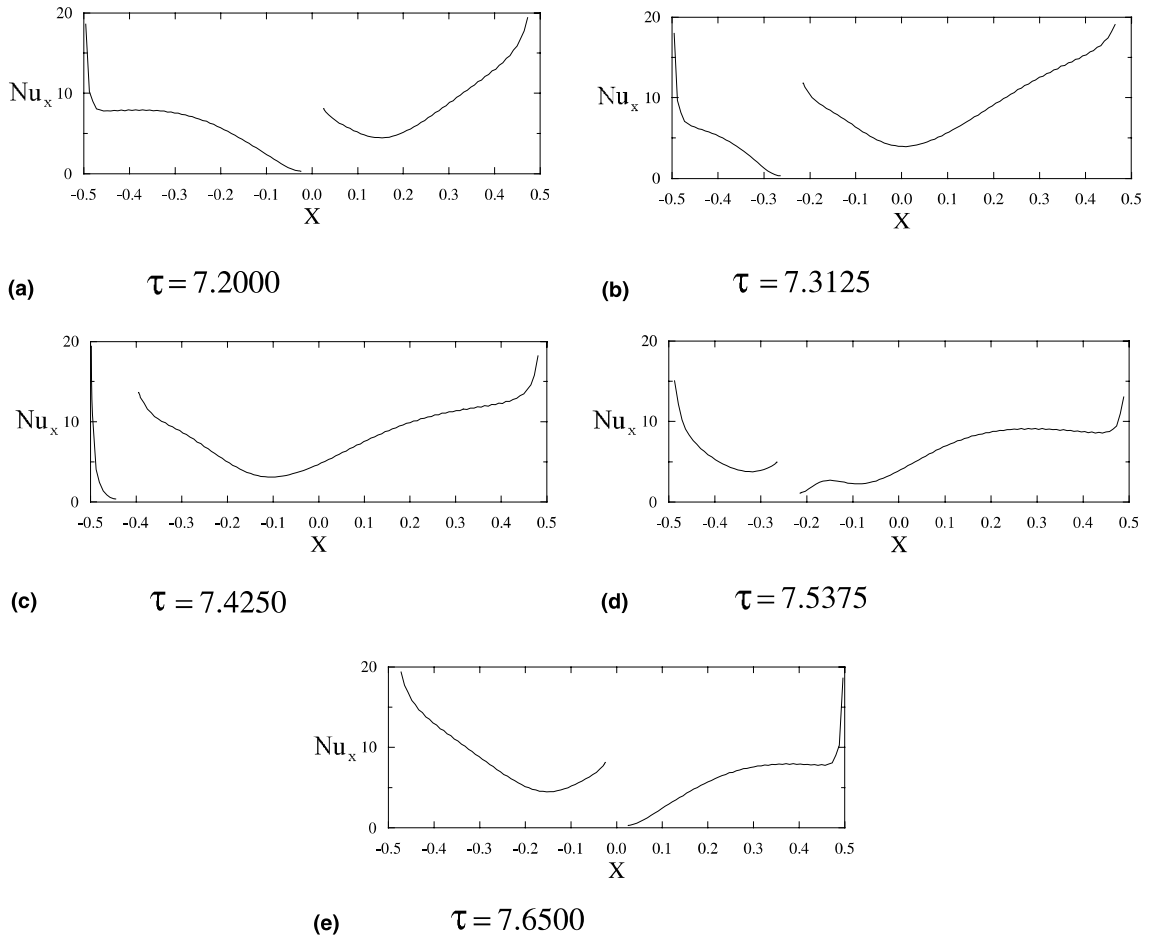

Fig. 8. The distributions of local Nusselt numbers on the heat plate for $R = 0.9$ under $Re_j = 100$, $U_b = 2.0$ and $D = 0.0$ cases.

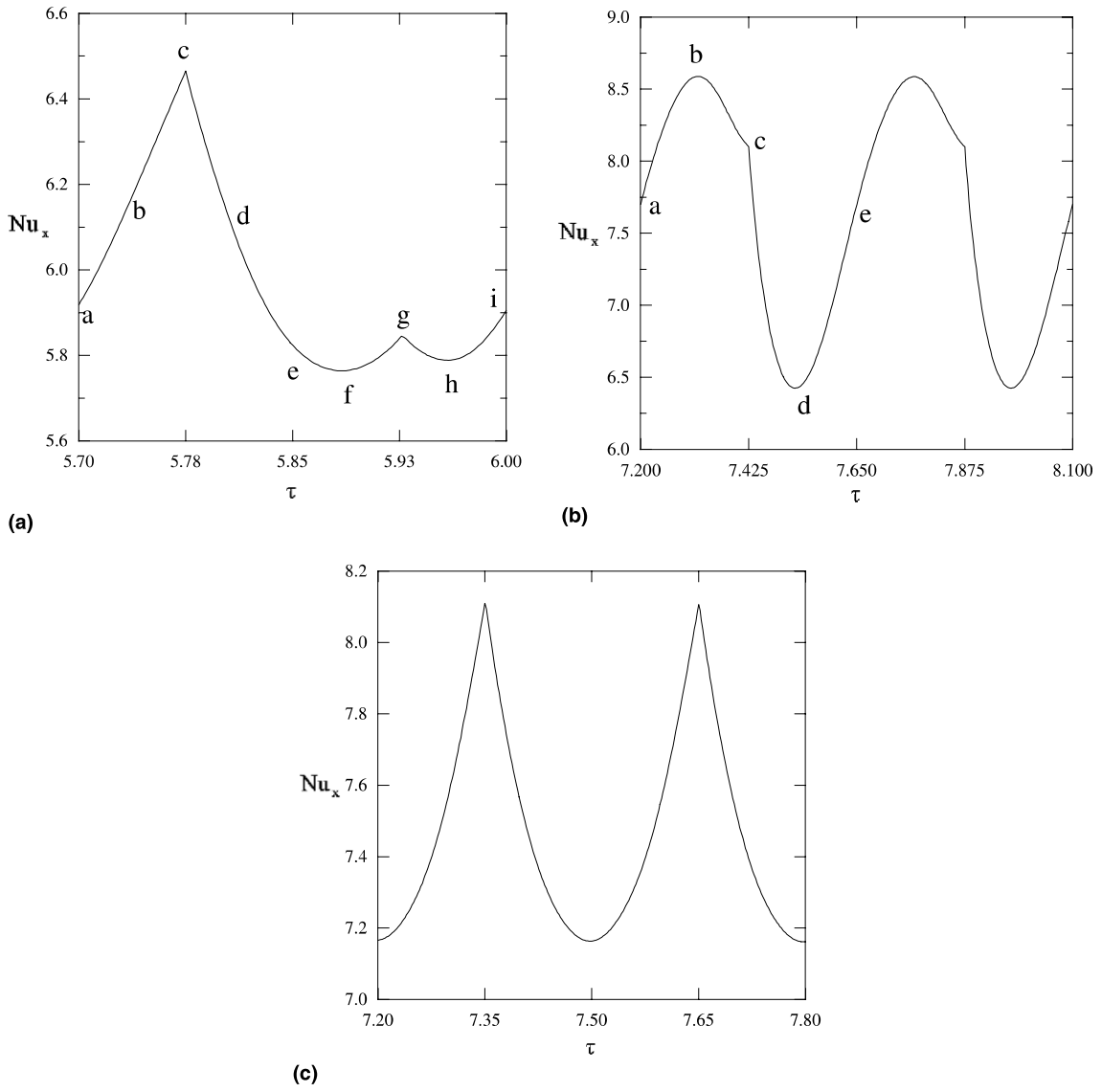

Fig. 9. The variation of the average Nusselt number $\overline{Nu_x}$ with τ for (a) $R = 0.3$, (b) $R = 0.9$ and (c) $R = 0.6$ under $Re_j = 100$, $U_b = 2.0$ and $D = 0.0$ cases.

increases behind the block by the reason mentioned above. The variation of average Nusselt number for $R = 0.3$ case is shown in Fig. 9(a). Since the moving distance is short, the appearance frequency of the moving block under the jet is relatively high. Then a recirculation zone induced by the moving block, which prevents chill fluids to flow toward the heat plate, always stays below the jet, and the local Nusselt number decreases. In addition, the variation of the flow field is drastic, then the variation of average Nusselt number needs longer moving distance to become a periodic state from point a to point i as shown in Fig. 9(a).

As for $R = 0.9$ case, when the block moves a stroke from the center point to the left side of the heat plate, chill fluids induced by the moving block flow to the heat plate and the local Nusselt number increases behind the moving block. As the block moves a stroke from the left side to the center point of the heat plate, the fluids pushed by the moving block interact the fluids discharged from the jet and the local Nusselt number decreases before the block. In the meanwhile, the increment of the local Nusselt number behind the block is indistinct because the new thermal boundary layer reforms in the wake of the moving block which causes the average Nusselt number to decrease. As the block

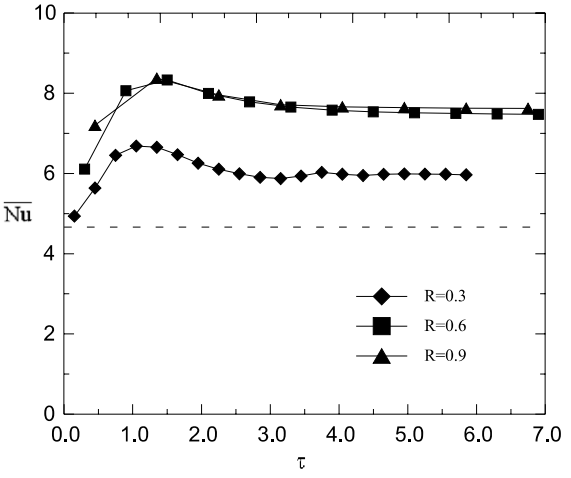

Fig. 10. The variations of time average Nusselt number per unit cycle $\overline{Nu}$ with τ for $Re_j = 100$, $U_b = 2.0$ and $D = 0.0$ case.

passes through the center of the heat plate and moves continuously to the right, the behaviors of the flow and thermal fields are similar to those of the block moving leftward at the same position. Then the variations of the average Nusselt number become periodic. Those phenomena are shown in Fig. 9(b).

For $R = 0.6$ case, the block moving distance is not short as $R = 0.3$ case, the trend of variation of average Nusselt number is similar to $R = 0.9$ case.

Fig. 10 shows the variations of time average Nusselt numbers per unit cycle $\overline{Nu}$ on the heat plate with the block moving distances R being 0.3, 0.6 and 0.9, respectively. The time average Nusselt number per unit cycle is defined as following equation:

$$\overline{Nu} = \frac{1}{T}\int_T \overline{Nu_x}\,d\tau, \tag{19}$$

where T is the dimensionless time per unit cycle.

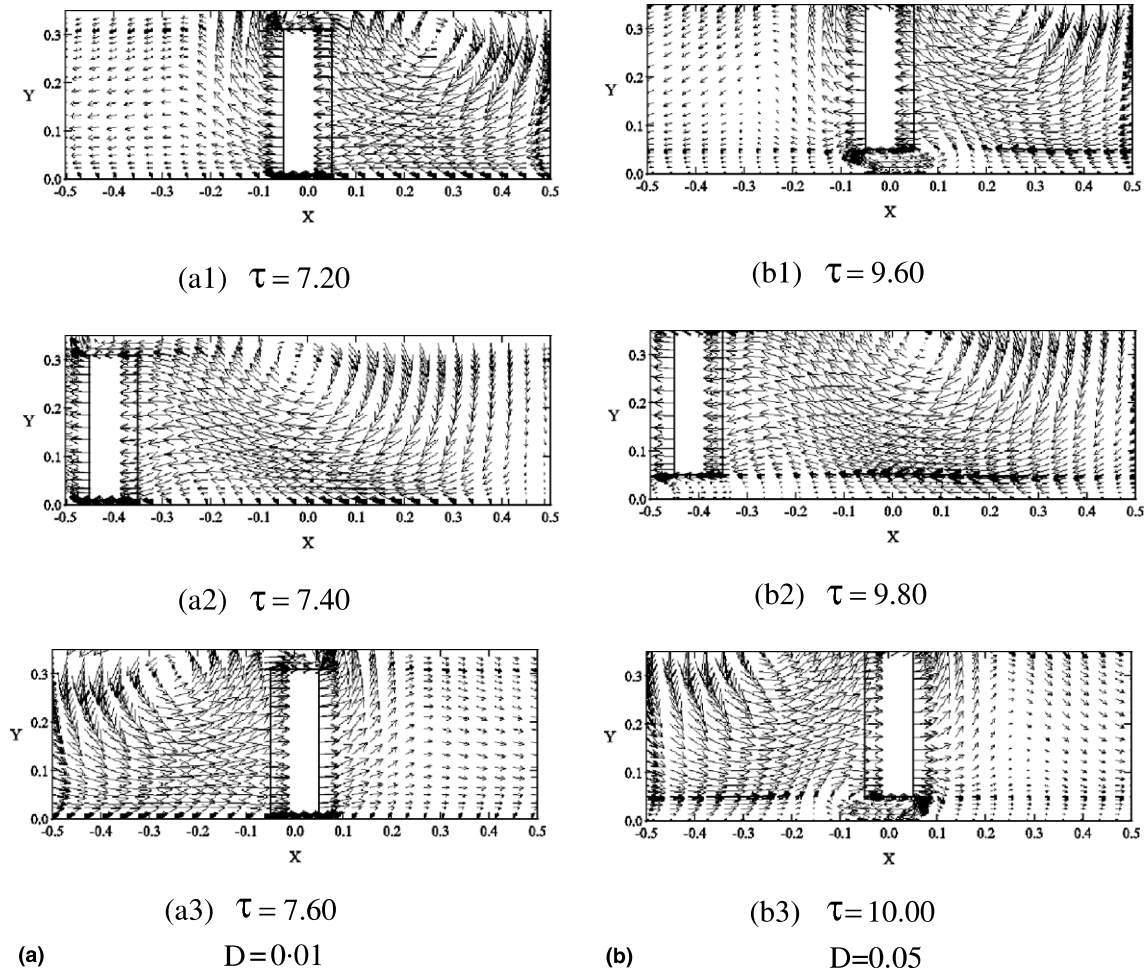

Fig. 11. The velocity vectors near the moving block for (a) $D = 0.01$ and (b) $D = 0.05$ under $Re_j = 100$, $U_b = 2.0$ and $R = 0.8$ cases.

The overline represents the time average Nusselt number of the heat plate when the block is stationary on the center of the heat plate.

Shown in Fig. 10, the time average Nusselt numbers per unit cycle are increased by the moving block about 23% in case $R = 0.3$, and 60% in cases $R = 0.6$ and 0.9. As the block moving distance R is larger than a certain distance, the effects of the interaction between the fluids discharged from the jet and the fluids induced by the moving block on the enhancement of heat transfer mentioned above become slight. This could cause the increment of heat transfer rate to be almost equal for $R = 0.6$ and 0.9 cases.

4.2. Vacant distance (D)

The variations of the velocities, constant thermal lines and local Nusselt numbers for $D = 0.0$, 0.01 and 0.05 under $Re_j = 100$, $U_b = 2.0$, and $R = 0.8$ are indicated in Figs. 11–13, respectively. These phenomena shown in Figs. 11–13 are in a certain period of reciprocation motions.

The velocity vectors near the moving block of $D = 0.01$ and 0.05 cases are shown in Fig. 11, while the block is moving from the center to the left point M of the heat plate.

The flow fields shown in Figs. 11(a1)–(a3) are case of $D = 0.01$. The vacant distance is small which causes the flow resistance to be large, and the fluids hardly pass through the vacant space. The fluids within the vacant space are drawn by the block and flow with the same direction of the moving block. The characteristics of the flow fields are similar to those ($D = 0.0$) shown in the present study [11].

The flow fields of the vacant distance being equal to 0.05 are shown in Figs. 11(b1)–(b3). The vacant space between block and heat plate is wide. The fluids, pushed by the block in the low region of block, could flow through the space independently. Then the directions of these fluids are opposite to that of the block, and a small recirculation zone is observed near the back low region of block. Therefore, these fluids passing through the vacant space prevent the other fluids induced by the block to flow toward the heat plate. As a result, an interaction zone exists on the heat plate, which is disadvantageous to the heat transfer of the heat plate.

Figs. 12–14 show the distributions of constant thermal lines of $D = 0.0$, 0.01 and 0.05, respectively. The variations of the constant thermal lines of $D = 0.01$ (Fig. 13) and 0.05 (Fig. 14) cases are different, since the fluids are hardly to flow through the vacant space of $D = 0.01$ case. The thermal boundary layer is hardly found out in the vacant space of $D = 0.01$ case with the magnitude of the constant thermal line shown in Fig. 13. On the contrary, a thin thermal boundary layer could be observed in the vacant space of $D = 0.05$ case shown in Fig. 14, and this layer has temperature gradient which induces the heat transfer of heat plate.

The distributions of local Nusselt number Nu_x of $D = 0.0$, 0.01 and 0.05 cases are shown in Figs. 15–17, respectively. The overline shown in Fig. 15(a) indicates the distribution of the local Nusselt number of the heat plate when the block is stationary on the center of the heat plate. Since fluids are difficult to pass through the

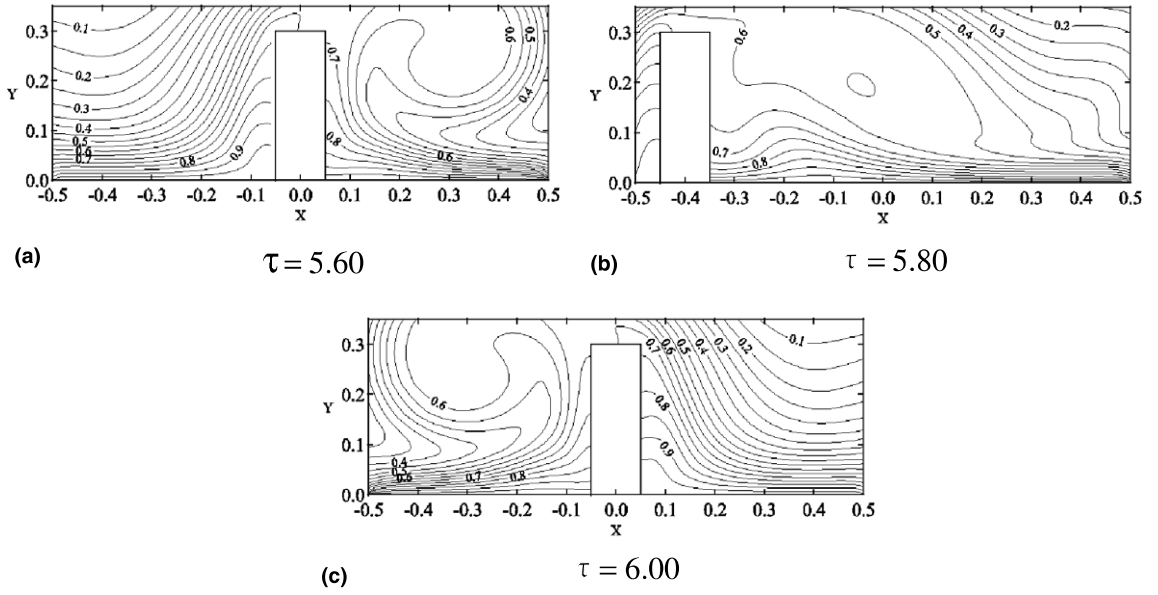

Fig. 12. The constant thermal lines near the moving block for $D = 0.0$ under $Re_j = 100$, $U_b = 2.0$ and $R = 0.8$ cases.

vacant space for $D = 0.01$ case, the flow fields of this case are similar to those of $D = 0.0$ case. As a result, the local Nusselt number on the region of heat plate right below the block is extremely small because of the temperatures of the fluids in the vacant space being almost equal to that of the heat plate shown in Fig. 16. Except the above region, chill fluids are induced by the moving block to flow to the other region of heat plate, and the distributions of local Nusselt number are similar to those of $D = 0.0$ case as shown in Fig. 15. As for $D = 0.05$ case, the local Nusselt number on the region of heat plate right below the block are larger than those of the above case of $D = 0.01$, because the thermal boundary layer exists on this region as shown in Fig. 17. The interaction phenomena already mentioned happen in the flow field and prevents chill fluids to flow toward

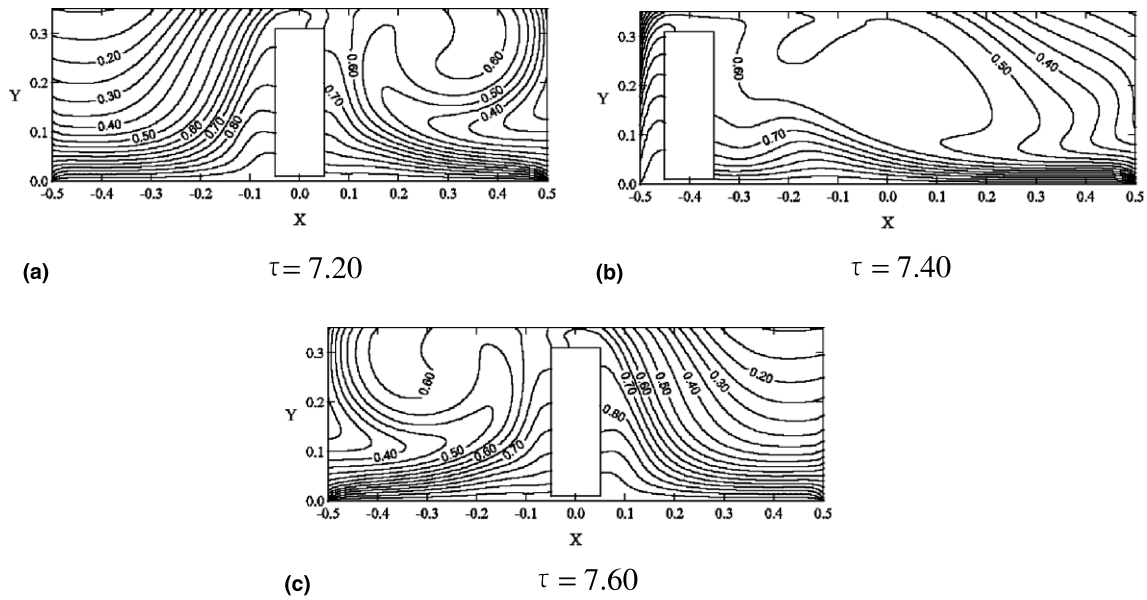

Fig. 13. The constant thermal lines near the moving block for $D = 0.01$ under $Re_j = 100$, $U_b = 2.0$ and $R = 0.8$ cases.

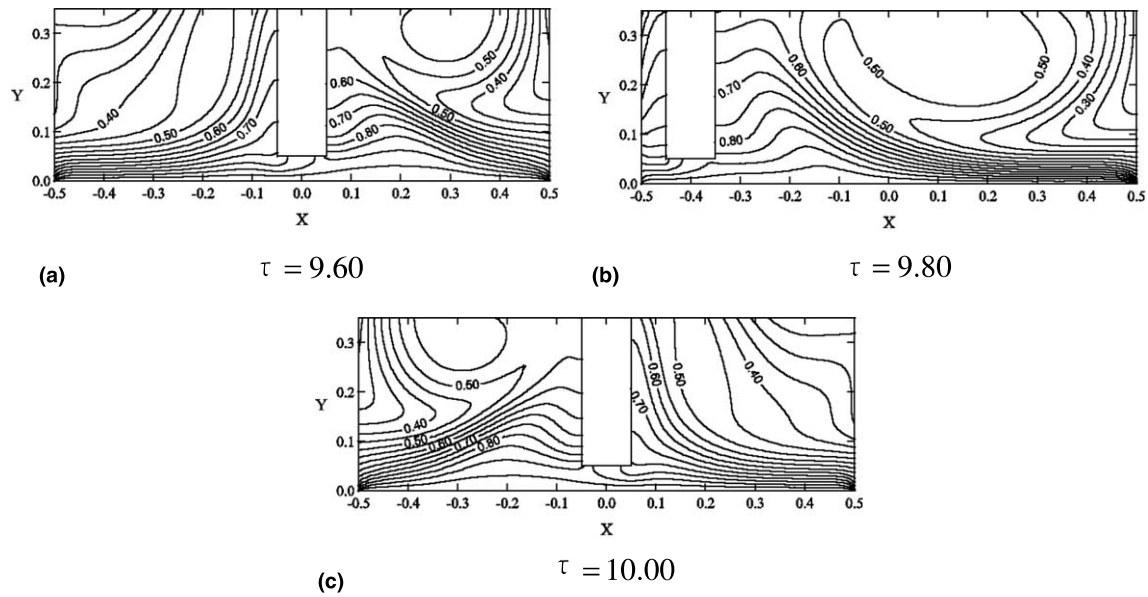

Fig. 14. The constant thermal lines near the moving block for $D = 0.05$ under $Re_j = 100$, $U_b = 2.0$ and $R = 0.8$ cases.

the heat plate. The distributions of local Nusselt number are then smaller than those of the $D = 0.01$ case.

Fig. 18 shows the variations of time average Nusselt numbers per unit cycle $\overline{Nu}$ on the heat plate with the vacant distances of 0.00, 0.01 and 0.05, respectively. The overline shown in Fig. 14 indicates the distribution of the time average Nusselt number per unit cycle of the heat plate when there is no block on the heat plate. The enhancements of the time average Nusselt number per unit cycle are about 16% in case $D = 0.05$, 22% in case $D = 0.01$ and 24% in case $D = 0.0$. When the block moves on the heat plate, the reformation of the

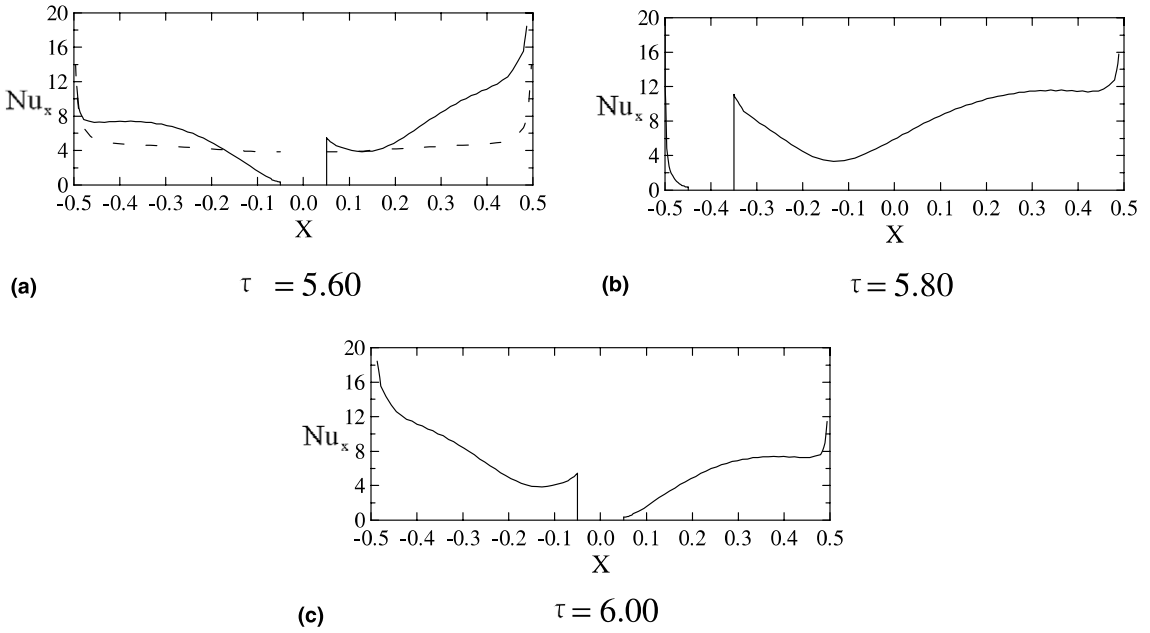

Fig. 15. The distribution of the local Nusselt numbers on the heat plate for $D = 0.0$ under $Re_j = 100$, $U_b = 2.0$ and $R = 0.8$ cases.

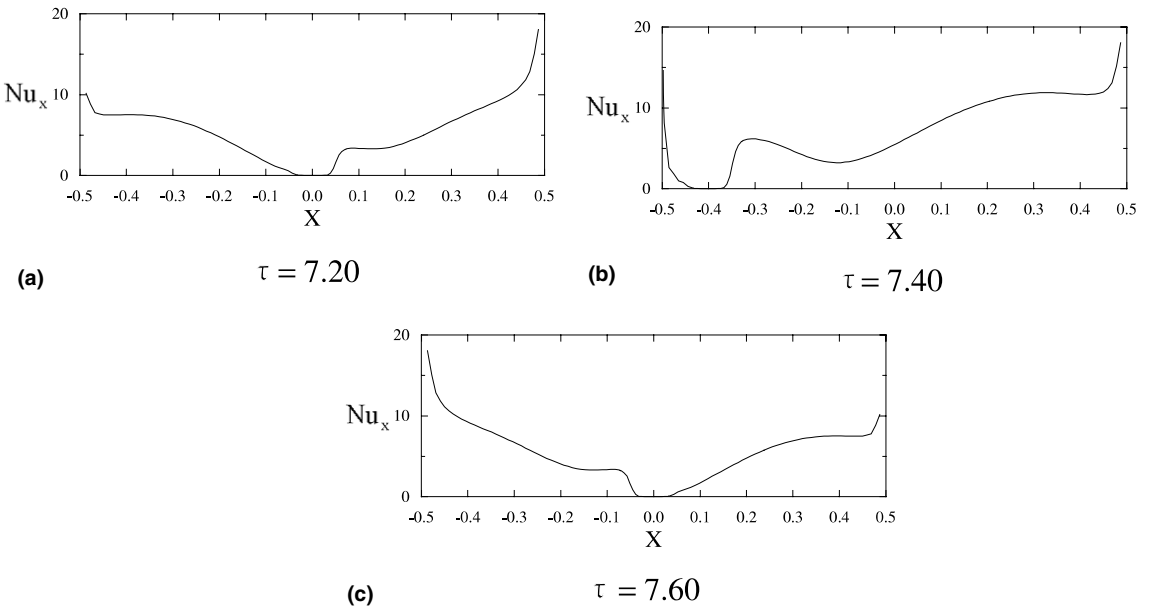

Fig. 16. The distribution of the local Nusselt numbers on the heat plate for $D = 0.01$ under $Re_j = 100$, $U_b = 2.0$ and $R = 0.8$ cases.

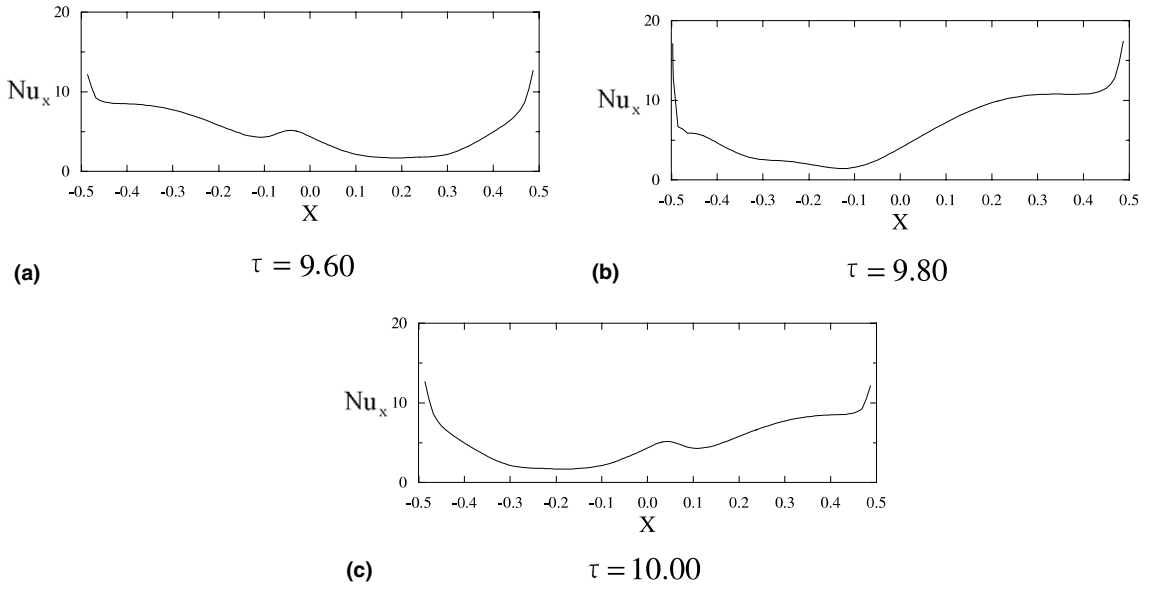

Fig. 17. The distribution of the local Nusselt numbers on the heat plate for $D = 0.05$ under $Re_j = 100$, $U_b = 2.0$ and $R = 0.8$ cases.

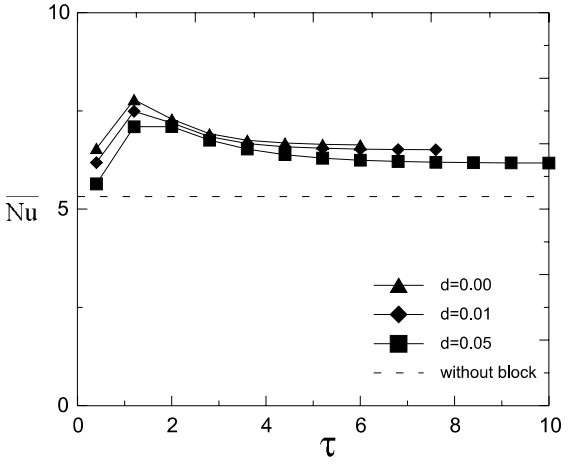

Fig. 18. The variations of time average Nusselt number per unit cycle $\overline{Nu}$ with τ for $Re_j = 100$, $U_b = 2.0$ and $R = 0.8$ case.

boundary layer right after the moving block is the main mechanism of the enhancement of heat transfer. The larger the vacant distance the reformation of boundary layer becomes difficult. This could cause heat transfer rate to be smaller. The maximum enhancement of heat transfer then occurs at case $D = 0.0$.

5. Conclusions

A numerical investigation of the two important parameters, block moving distance and vacant distance between block and heat plate, for heat transfer of a block moving back and forth on a heat plate under a slot jet is studied. The main conclusions can be summarized as follows:

1. The increment of the heat transfer rate by the block moving on the heat plate is not directly proportional to the block moving distance (R).
2. For obtaining more heat transfer rate, the small vacant distance is expected.

Acknowledgements

The support of this work by National Science Council, Taiwan, ROC, under contract 89-2212-E-009-072 is gratefully acknowledged.

References

[1] A.E. Bergles, Recent development in convective heat-transfer augmentation, Appl. Mech. Rev. 26 (1973) 675–682.
[2] A.E. Bergles, Survey and evaluation of techniques to augment convective heat and mass transfer, Progr. Heat Mass Transfer 1 (1969) 331–424.
[3] A.S. Mujumdar, W.J.M. Douglas, Impingement heat transfer: a literature survey, in: TAPPI Meeting, SM 8603.7, NO, 1972, pp. 107–136.
[4] H. Martin, Heat and mass transfer between impinging gas jets and solid surfaces, in: T. Irvine, J.P. Harnett (Eds.), Advances in Heat Transfer, vol. 13, Academic Press, New York, 1977, pp. 1–60.
[5] K. Jambunathan, E. Lai, M.A. Moss, B.L. Button, A review of heat transfer data for single circular jet

impingement, Int. J. Heat Mass Transfer 13 (2) (1992) 106–115.
[6] Y.J. Chou, Y.H. Hung, Impingement cooling of an isothermally heated surface with a confined slot jet, ASME. J. Heat Transfer 116 (1994) 479–482.
[7] W.M. Chakroun, A.A. Abdel-Rahman, S.F. Al-Fahed, Heat transfer augmentation for air jet impinged on a rough surface, Appl. Thermal Eng. 18 (1998) 1225–1241.
[8] Y.S. Chung, D.H. Lee, J.S. Lee, Heat transfer characteristics of an axisymmetric jet impinging on the rib-roughened convex surface, Int. J. Heat Mass Transfer 42 (1999) 2101–2110.
[9] D.A. Zumbrunnen, M. Aziz, Convective heat transfer enhancement due to intermittency in an impinging jet, ASME. J. Heat Transfer 115 (1993) 91–98.
[10] Y. Haneda, Y. Tsuchiya, K. Nakabe, K. Suzuki, Enhancement of impinging jet heat transfer by making use of mechano-fluid interactive flow oscillation, Int. J. Heat Fluid Flow 19 (1998) 115–124.
[11] W.-S. Fu, K.-N. Wang, W.-W. Ke, An investigation of a block moving back and forth on a heat plate under a slot jet, Int. J. Heat Mass Transfer 44 (2001) 2621–2631.
[12] W.S. Fu, S.J. Yang, Numerical simulation of heat transfer induced by a body moving in the same direction as flowing fluids, Heat Mass Transfer 36 (2000) 257–264.
[13] A.R.P. van Heiningen, A.S. Mujumdar, W.J.M. Douglas, Numerical prediction of the flow field and impingement heat transfer caused by a laminar slot jet, ASME. J. Heat Transfer 98 (1976) 654–658.